Journal of Data Acquisition and Processing
ISSN: 1004-9037
https://sjcjycl.cn/
DOI: 10.5281/zenodo.7546553

THE DEVELOPMENT OF SITE-SPECIFIC RESPONSE SPECTRA FOR SOUTH COTABATO, PHILIPPINES

Warda Panondi[1*], Israel A. Baguhin[2]
[1*]Mindanao State University-Main Campus, Marawi City Lanao Del Sur, 9700 Philippines
[2]University of Science and Technology of Southern Philippines Lapasan, Cagayan de Oro City, 9000 Philippines
***Corresponding Author:** Warda Panondi
[*]Mindanao State University-Main Campus, Marawi City Lanao Del Sur, 9700 Philippines

ABSTRACT
Adequate and timely seismic hazard assessment in an earthquake-prone country like the Philippines is essential. Earthquakes in South Cotabato have underlined the phenomenological influence of local geological conditions on levels of damage and the resultant loss of life. The advancement of suitable earthquake-resistant structures through reliable ground motion prediction utilizing seismic provision and site-specific investigation can reduce life losses and damages from a devastating earthquake. This study developed a site-specific response spectrum in the Municipality of South Cotabato using a Probabilistic Seismic Hazard Analysis approach. The R-CRISIS, Z-Map, and ArcGIS are the tools used to generate the result utilizing earthquake catalog from DOST-PHIVOLS and USGS as inputs in the model. The work revealed that t=0.01s, Municipalities of Banga, Koronal City, Lake Sebu, Norala, Santo Niño, Surallah, and Tantangan transcend the value of spectral acceleration using at t= 0.00 s of NSCP response spectrum of 0.4g by 0.466g, 0.451g, 0.437g, 0.492g, 0.48g, 0.44g, and 0.489g respectively. On the other hand, General Santos City, Polomolok, T'Boli, Tampakan, and Tupi is a lesser value than of NSCP response spectrum at t=0.01s by 0.34g, 0.316g, 0.379g, 0.383g, and 0.340g, respectively. The response spectrum developed from the PSHA generally provides a better response spectrum for site response analysis. The study's result is a useful reference to the structural engineer or any project implementing agency to establish infrastructure in South Cotabato Region. Furthermore, the results maximized as a basis for the future development of structural engineering in the Province and the first step toward developing site-specific spectral shapes for earthquake engineering applications in the Philippines.
Keyword: Seismic Hazard Analysis, PSHA, site-specific response spectrum, R-CRISIS, ZMAP

1. INTRODUCTION
Earthquake is one of the most dangerous natural hazards because of the tectonic plate's continuous movement that releases elastic energy in terms of waves (Adagunodo & Sunmonu, 2015). The Philippines is prone to natural hazards, with an average of 20 typhoons and 100 to 150 events of earthquakes occurred annually. For instance, the country was ranked as 1st place as the most exposed to natural hazards and a vulnerable position in the world in 2022 due to its geographical location (WRR, 2022). With this, adequate and timely seismic hazard assessment in an earthquake-prone area like the Philippines is essential.

The effect of insufficient reliable seismic hazard analysis and site-specific design criteria in seismic hazards zone may cause a severe harmful disastrous event that will damage the communities, environment, and economy. On the other hand, the advancement of suitable earthquake-resistant structures through reliable ground motion prediction utilizing seismic provision and site-specific investigation can reduce life losses and damages from the devastating earthquake (Kalkan et al., 2004).

Recently, earthquakes in South Cotabato have underlined the phenomenological influence of local geological conditions on levels of damage and the resultant loss of life. In the aftermath of these events, most of the detrimental effects were affected in areas underlain by soft soil deposits. These damaged concentrations have accentuated the essential need to develop site-specific response spectra for estimating ground motions in terms of magnitude, distance, and local site conditions using the Probabilistic Seismic hazard Analysis or PSHA (Baguhin and Orejudos, 2020). By this scenario, the response spectra for earthquake hazard mapping emphasized the importance of seismic hazard assessment. In earthquake hazard analysis, deterministic and probabilistic approaches are generally used to develop the site-specific response spectrum.

In this study, the researcher utilized the PSHA based on Cornell, 1968. The PSHA determines seismic design load for the design of structure because of practical and widely used techniques to inspect the probabilistic limit of uncertainties in the size, location, recurrence rate of earthquakes, and ground motion characteristics explicitly considered for the evaluation of seismic hazard. Also, the PSHA provides a context in which these uncertainties can identify and quantified (Anbazhagan, 2017). Exploring the relationship between the general characteristics of spectral shapes derived from vital ground motion records and the parameters affecting them was appeared possible because of the increasing number of records available in the Philippines.

The updated database, analyses, information, and related result of previous studies were investigated, harmonized, and considered to ensure the results' reliability. Furthermore, this study aims to provides a general framework for developing estimates of site-specific response spectra in each Municipality of South Cotabato based on specific parameters characterizing the earthquake magnitude, geology of the Province, and the distance between source and site with associated measures of uncertainty. The R-CRISIS, Z-Map, and ArcGIS were utilized in this research to generate the inputs and terrain analysis algorithm. Moreover, this study's results will be verified and compared to the National Structural Code of the Philippines (NSCP).

This study's results can be a useful reference to the structural engineer or any project implementing agency for establishing infrastructure in South Cotabato Region. Furthermore, the results maximized as a basis for the future development of structural engineering in the province and the first step toward developing site-specific spectral shapes for earthquake engineering applications in the Philippines.

2. METHODOLOGY

2.1. Study Area

The Province of South Cotabato was located in the Southern part of Mindanao with a coordinate system of 6.3358 N 124.7741 E. In this study, the considered area of responsibility was South Cotabato, which is composed of 12 Municipalities such as Tupi, Tantangan, Tampakan, T'Boli, Surallah, Santo Nino, Polomolok, Norala, Lake Sebu, Koronadal City, Banga, and General Santos that presented in *Figure 1*. Moreover, the area of influence was measured by taking a 250 km area around the South Cotabato boundary. This area was assumed to influence the area of responsibility by the occurrence of any earthquake activity.

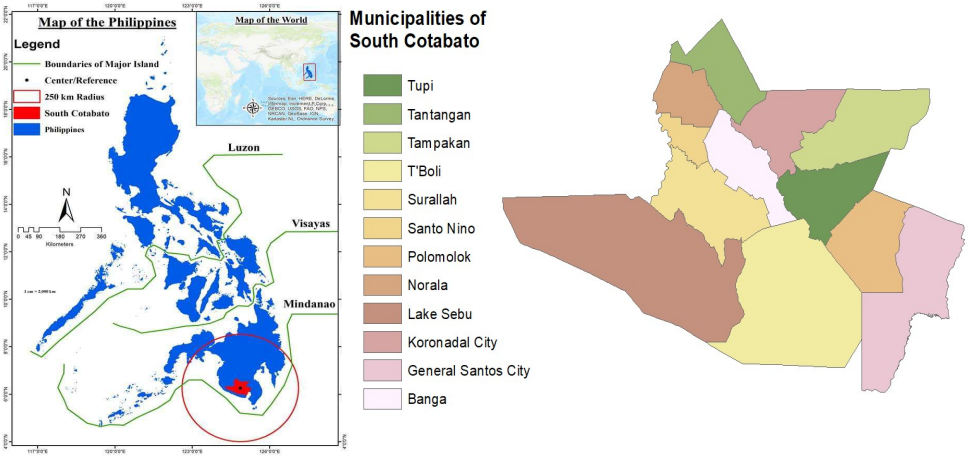

***Figure 1**. Study Area. Area of the Influence consideration (leftside) and area of Responsibility (rightside).*

2.2. Earthquake Catalogue and Soil Test Report

The earthquake catalog in this study was retrieved from the Department of Science and Technology – Philippines Institute of Volcanology and Seismology (DOST-PHIVOLCS) (https://www. phivolcs.dost.gov.ph/) and United States Geological Survey (USGS) (https://earthquake.usgs.gov/). Moreover, the soil test report was retrieved from the Department of Public Works and Highways (DPWH) – Region 12. The SPT-N values of 23 boreholes in South Cotabato distributed in every Municipality was correlated to predict the average upper 30-m shear wave velocity.

2.3. Homogenization of Earthquake Catalogue

In this study, earthquake events were homogenized (Ahmad, 2016) by converting the events into moment magnitude to have a uniform and single magnitude type. The surface-wave magnitude (M_s), body-wave magnitude (M_b), and local magnitude (M_L) will be converted to moment magnitude (M_w) using the derive conversion equation of (Waseem 2016) as shown in *Table 1*.

***Table 1.** Correlation of earthquake magnitude to M_w (Waseem, 2016)*

No.	Relationship Type	Conversion Equation
1	Mw ≤ 6.2	Mw= 0.535Ms + 2.69
2	Mw >6.2	Mw= 0.895Ms + 0.53

3	Mw and Mb	Mw = Mb + 0.103
4	Mw and ML	Mw = 0.878ML + 0.838

2.4. Ground Motion Prediction Equation (GMPE)

GMPE has a significant part in hazard calculation by defining the uncertain ground-motion amplitudes for each rupture scenario (Bajaj & Anbazhagan, 2019). In this study, (Atkinson & Boore, 2006) was used as the attenuation model pre-defined in R-CRISIS software (Ordaz & Salgado-Gálvez, 2017).

2.5. ZMAP and R-CRISIS software

ZMAP is software used in the analysis of the seismicity pattern (Wyss et al., 2001). The algorithm of (Gardner & Knopoff, 1974) was generally used in the ZMAP software run in Matlab (Ahmad, 2016). In this study, ZMAP was utilized to de-clustering the earthquake catalog data to remove the catalog's dependent events such as; foreshocks and aftershocks from the record (Ahmad, 2016). Likewise, the ZMAP software was mainly used to determine the seismic parameter value "a" and "b" from Gutenberg-Richter (GR) law that presented in (4). Moreover, R-CRISIS is the tool utilized to perform probabilistic seismic hazard analyses (Ordas & Salgado-Gálvez., 2017). The R-CRISIS software was mainly used to develop a site-specific response spectrum.

$$\lambda_{\alpha,\beta,Mo,Mmax} = e^{(\alpha-\beta M_o)}\left[e^{-\beta(M-M_o)} - e^{-\beta(M_{max}-M_o)}\right]\left[\frac{1}{1-e^{-\beta(M_{max}-M_o)}}\right] \quad (1)$$

$$\alpha = a\, x \ln 10 \quad (2)$$

$$\beta = b\, x \ln 10 \quad (3)$$

$$log\ \lambda_m = a - bM_w \quad (4)$$

3. RESULT AND DISCUSSION

3.1 De-clustering of Earthquake Catalog using ZMAP Software

The earthquake catalog consists of 5,693 earthquake moment magnitude events. After de-clustering using the Reasenberg Method in ZMAP software, the earthquake catalog was reduced to 4,311-moment magnitude events, as shown in *Figure 2*.

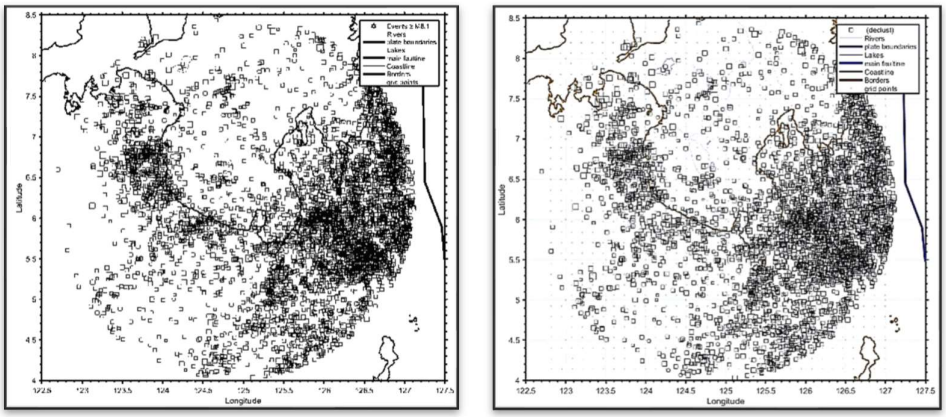

(a) **(b)**

Figure 2. *Seismicity of the study area with 250-km radius (a) before de-clustering and (b) after de-clustering*

The earthquake catalog within the 250-km radius of influence, containing 5693 and 4311-moment magnitude earthquakes before and after de-clustering, was presented in *Figure 2*. Aftershocks and foreshocks are temporally and spatially dependent on the mainshocks, de-clustering was carried out to remove the dependent events from the catalog. Seismicity interacts among adjacent tectonic contexts (i.e., interface mainshocks can trigger crustal aftershocks), several domains were de-clustered together. Then earthquakes were classified into de-clustered sub-catalogs. The two de-clustering groups were a crustal, interface, and shallow slab seismicity (which lies laterally beneath the interface) and deep slab. The de-clustering of the algorithm works in two spatial dimensions, comparing epicenters and not hypocenters. Thus, for steep subduction geometry, where much of the deep slab would occupy the triggering window for large interface or crustal earthquakes, this distinction between the two groups is critical (Johnson et al., 2020).

3.2 Seismic Source Parameters

The ZMAP software was used for calculating the a-value and b-value parameters shown in *Figure 3*. The *Figure 3* shows the study area's b-value maps using the 0.05° x 0.05° grid cells within the 250-km radius of the area influence. The grid cell numerical values, such as frequency- magnitude distribution plot as shown in the left bottom of *Figure 3*, of every fault line, were taken.

The output value from the ZMAP of every seismic source was brought into the average value and recorded, as shown in *Table 2*. The seismic parameters "a" and "b" value, α, β, and $\lambda_{\alpha,\beta,Mo,Mmax}$ were also calculated using **(1)**, **(2)**, and **(3)** as summarized in *Table 2*.

The seismic parameters of all sources were presented in *Table 2*. The a-value is a constant, and the b-value is the ratio of small to large-moment magnitude earthquakes that determines the relative number of earthquakes of different magnitude. Seismic hazard analysis is having a high sensitivity to b-value (Felzer, 2006). The higher the a-value, the seismicity of the area is also getting higher. Moreover, small moment magnitude earthquakes occur often compare the large events when the b-value is more than 1.0 (Baguhin & Orejudos, 2020). In *Table 2*, eight (8) seismic sources have a b-value less than 1.0 out of twenty-one (21) seismic sources. High moment magnitudes

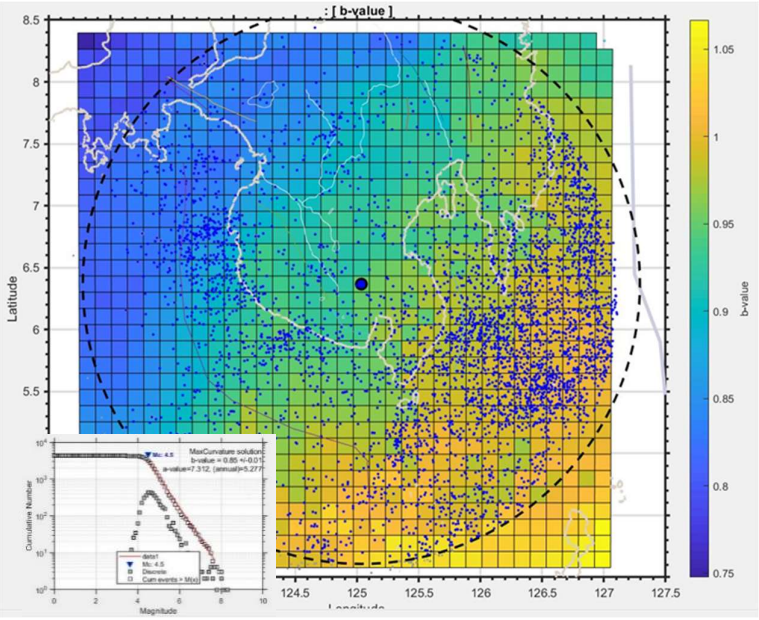

Figure 3. *The "b" value maps of South Cotabato with frequency-magnitude distribution plot using the ZMAP software*

are in the Cotabato trench, Central Mindanao fault, Agusan Marsh, MF Daguma Ext., MF Mindanao Ext., Zone 1, Zone 5, and Zone 8.

Furthermore, the annual rate of occurrence ($\lambda_{\alpha,\beta,Mo,Mmax}$) of the Davao river has the highest value of 142.25 events per year followed by MF Western Mindanao Ext., Zone 2, Tagbulan Fault, Davao Fault, Zone 8, and Cotabato Trench that has value of 98.12, 33.87, 33.82, 33.13, 28.92 and 27.12, respectively. Also, Colosas Fault, Zone 7, Zone 5, Zone 6, Mati Segment, Lanao, MF Daguma Ext., Zone 4, Zone 1, Zone 3, Caraga River, Compostella Valley, Central Mindanao Fault, and Agusan Marsh have a mean annual rate of occurrence of 25.19, 25.19, 24.75, 22.95, 22.0, 21.03, 20.30, 13.12, 12.21, 12.03, 11.40, 10.57, 9.32 and 9.06, respectively.

Table 2. *Seismic parameters for all sources.*

Seismic sources/Fault	a	b	α	β	$\lambda_{\alpha,\beta,Mo,Mmax}$
Cotabato Trench	5.99	0.97	13.80	2.23	27.12
Mati Segment	6.20	1.05	14.28	2.41	22.00
Caraga River	5.74	1.01	13.22	2.30	11.40
Compostella Valley	5.85	1.06	13.47	2.44	10.57
Central Mindanao Fault	3.02	0.52	6.95	1.20	9.32
Agusan Marsh	5.24	0.91	12.08	2.10	9.06
Colosas Fault	7.78	1.36	17.93	3.12	25.19
Davao Fault Zone	6.20	1.02	14.28	2.35	33.13

Table 2. *Seismic parameters for all sources. (Continuation)*

Seismic sources/Fault	a	b	α	β	$\lambda_{\alpha,\beta,Mo,Mmax}$
Tagbulan	6.32	1.07	14.56	2.46	33.82
Cotabato Trench	5.99	0.97	13.80	2.23	27.12
Mati Segment	6.20	1.05	14.28	2.41	22.00
Caraga River	5.74	1.01	13.22	2.30	11.40
Compostella Valley	5.85	1.06	13.47	2.44	10.57
Central Mindanao Fault	3.02	0.52	6.95	1.20	9.32
Agusan Marsh	5.24	0.91	12.08	2.10	9.06
Colosas Fault	7.78	1.36	17.93	3.12	25.19
Davao Fault Zone	6.20	1.02	14.28	2.35	33.13
Tagbulan	6.32	1.07	14.56	2.46	33.82
Cotabato Trench	5.99	0.97	13.80	2.23	27.12
Mati Segment	6.20	1.05	14.28	2.41	22.00
Caraga River	5.74	1.01	13.22	2.30	11.40
Compostella Valley	5.85	1.06	13.47	2.44	10.57
Central Mindanao Fault	3.02	0.52	6.95	1.20	9.32
Agusan Marsh	5.24	0.91	12.08	2.10	9.06
Colosas Fault	7.78	1.36	17.93	3.12	25.19
Davao Fault Zone	6.20	1.02	14.28	2.35	33.13
Tagbulan	6.32	1.07	14.56	2.46	33.82
MF Daguma Ext.	5.52	0.93	12.72	2.13	20.30
Lanao	1.05	6.16	14.19	2.42	21.03
Davao River	6.98	1.04	16.07	2.40	142.25
Western Mindanao Ext.	5.95	0.88	13.70	2.03	98.12
Zone 1	5.41	0.95	12.45	2.20	12.21
Zone 2	6.32	1.07	14.56	2.46	33.87
Zone 3	7.75	1.48	17.85	3.40	12.03
Zone 4	6.81	1.26	15.69	2.90	13.12
Zone 5	5.21	0.85	12.00	1.95	24.75
Zone 6	6.00	1.02	13.83	2.34	22.95
Zone 7	7.78	1.37	17.93	3.12	25.19
Zone 8	4.68	0.68	10.77	1.56	28.92

3.3 Shear Wave Velocities (Vs_{30})

The Vs_{30} defined as the average seismic shear-wave velocity from the surface to a depth of 30 meters, has found widespread use as a parameter to characterize local site response for a wide variety of applications ranging from simplified earthquake resistant design procedures in building codes to regional and global seismic hazard mapping. Correlations with other local site characteristics, including V_{sz} measured to different depths, have shown Vs_{30} to be a robust parameter for characterizing local site response for many applications (Borcherdt, 2010). Standard Penetration Test N-Value (SPT-N) was correlated using Kumar, Anbazhagan, and

Sitharam (2010) (Nbazhagan et al., 2013)(Jhinkwan & Jain, 2016) expressed in **(5)** to get shear-wave velocities at different depths. Thus, **(6)** and *Table 3* (Boore et al., 2011) were used to predict average upper 30-meter shear-wave velocities (Vs30) of different soils. Finally, using the IDW Interpolation Method of the ArcGIS software, a .tiff file was created and converted to a .grd file in Surfer software for Vs30 values, as shown in *Table 4*.

$$Vs = 73.381\, N^{0.489} \text{ (for all soil)} \qquad \textbf{(5)}$$

$$\log V_{s30} = c_{oE}\delta_{E+}\, c_o + c_1 log V_{Sz} + c_2 (log V_{Sz})^2 \qquad \textbf{(6)}$$

Table 3. *Coefficient of Equation 6 relating to $logV_{s30}$ and $logV_{Sz}$ without regard to Site class (Boore et al., 2011)*

Depth, z	c_o	c_1	c_2	σ_{RES}
5	0.2046	1.318	-0.1174	0.119
6	-0.06072	1.482	-0.1423	0.111
7	-0.2744	1.607	-0.16	0.103
8	-0.3723	1.649	-0.1634	0.097
9	-0.4941	1.707	-0.1692	0.09
10	-0.5438	1.715	-0.1667	0.084
11	-0.6006	1.727	-0.1649	0.078
12	-0.6082	1.707	-0.1576	0.072
13	-0.6322	1.698	-0.1524	0.067
14	-0.6118	1.659	-0.1421	0.062
15	-0.578	1.611	-0.1303	0.056
16	-0.543	1.565	-0.1193	0.052
17	-0.5282	1.535	-0.1115	0.047
18	-0.496	1.494	-0.102	0.043
19	-0.4552	1.447	-0.09156	0.038
20	-0.4059	1.396	-0.08064	0.035
21	-0.3827	1.365	-0.07338	0.03
22	-0.3531	1.331	-0.06585	0.027
23	-0.3158	1.291	-0.05751	0.023
24	-0.2736	1.25	-0.04896	0.019
25	-0.2227	1.202	-0.03943	0.016
26	-0.1768	1.159	-0.03087	0.013
27	-0.1349	1.12	-0.0231	0.009
28	-0.09038	1.08	-0.01527	0.006
29	-0.04612	1.04	-0.007618	0.003

Table 4. *V_{s30} values in South Cotabato, Philippines*

Sites	**Vs30 (m/s)**
Banga	397.9
General Santos City	502.54

Koronadal City	412.46
Lake Sebu	407.52
Norala	399.47
Polomolok	531.57
Santo Nino	395.27
Surallah	408.89
T'Boli	447.73
Tampakan	465.92
Tantangan	398.93
Tupi	509.2

The highest shear-wave velocity is Polomolok with a value of 531.57 m/s, followed by Tupi of 509.2 m/s, General Santos City of 502.54 m/s, Tampakan of 465.95 m/s, T'Boli of 447.73 m/s, Koronadal City of 412.46 m/s, Surallah of 408.89 m/s, Lake Sebu of 407.52 m/s, Norala of 399.47 m/s, Tantangan of 398.93, Banga of 397.9 and lastly, Santo Nino 395.27 m/s as shown in *Table 4.*

3.4 Site Specific Response Spectrum

The R-CRISIS 2015 software was utilized to develop site-specific response spectra in South Cotabato, Philippines. The procedure conducted using the R-CRISIS software was shown in Figures 4 to Figure 9.

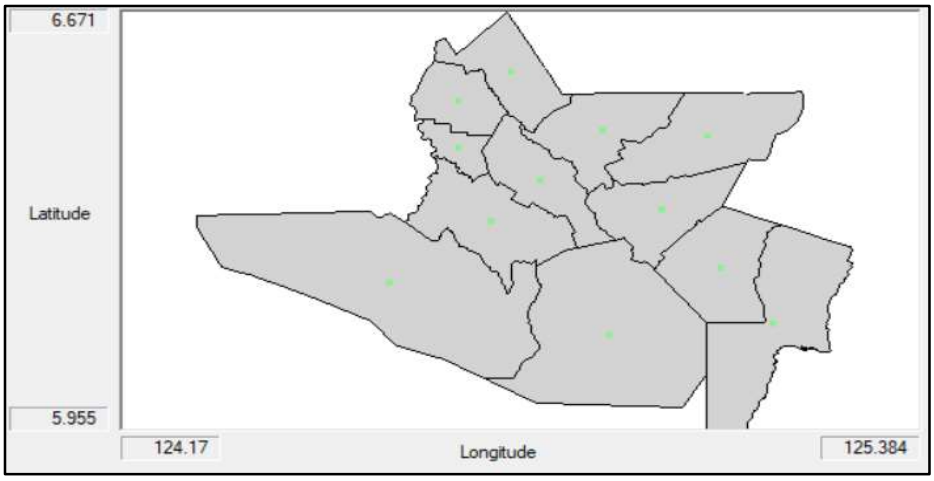

Figure 4. *Map and City files*

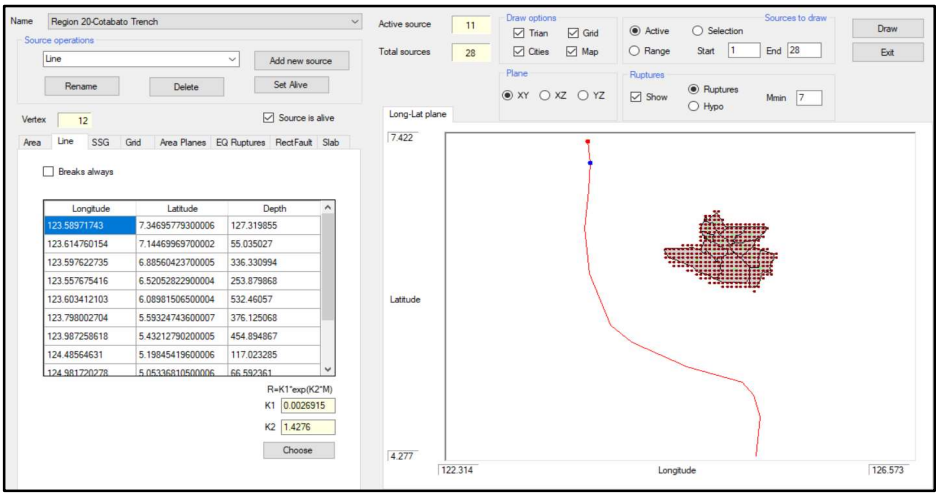

Figure 5. *Seismic source geometry*

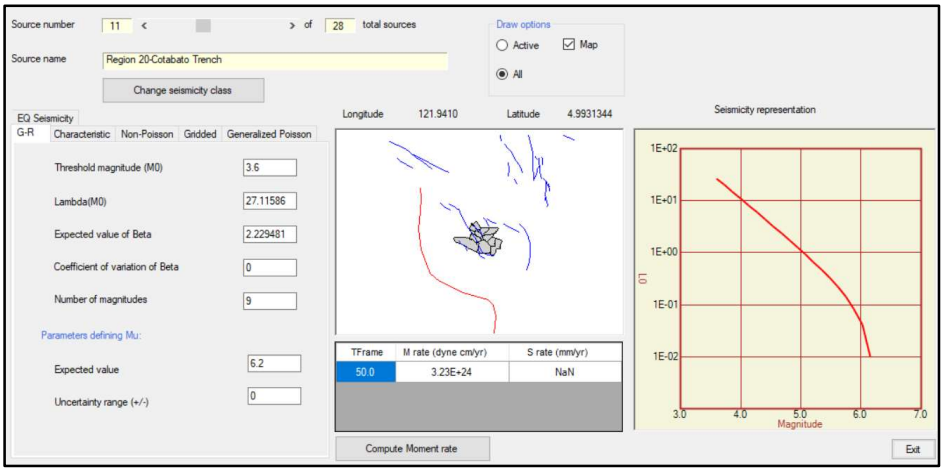

Figure 6*. Source Seismicity*

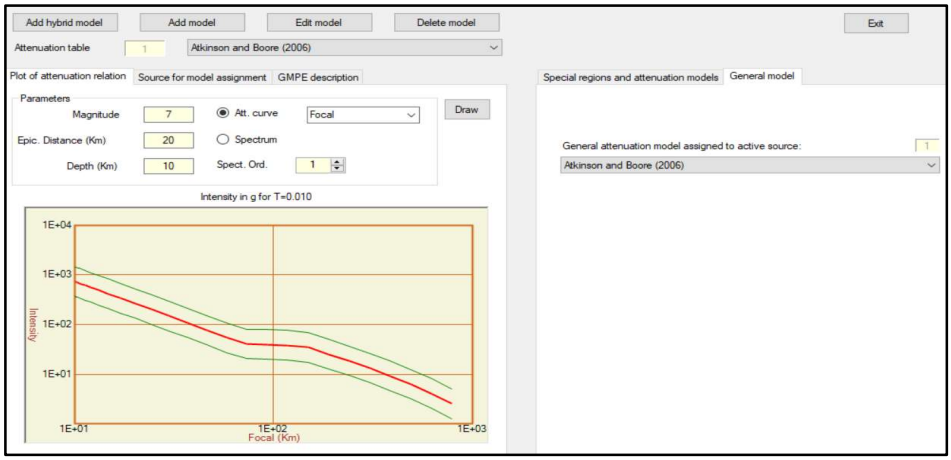

Figure 7*. Attenuation equation definition*

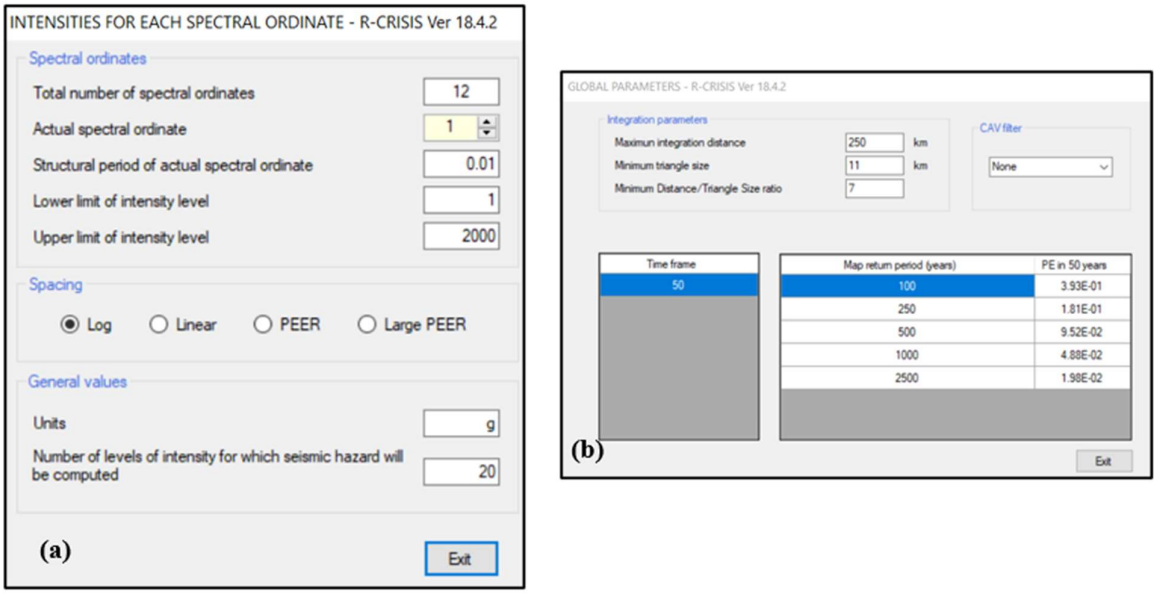

Figure 8. *(a) Spectral coordinates definition and (b) Global parameters definition*

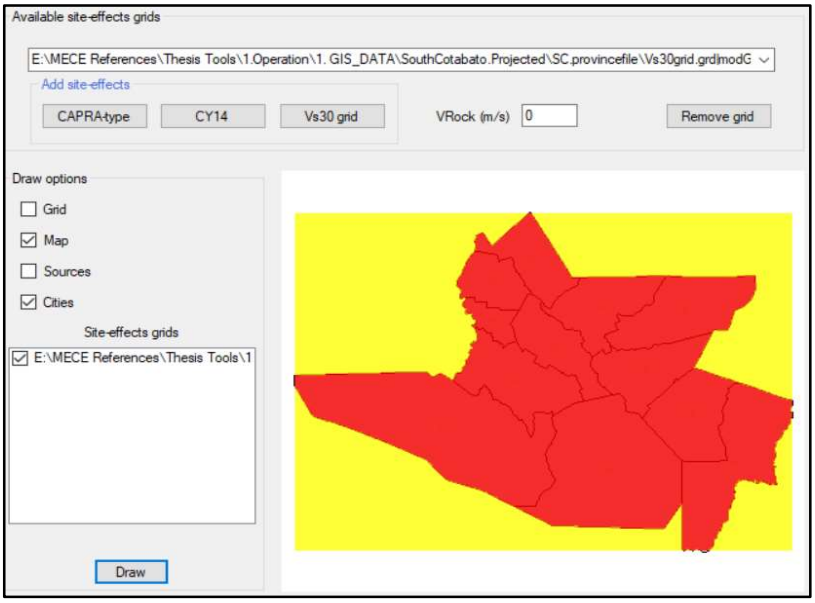

Figure 9*. Site effects of local soil condition*

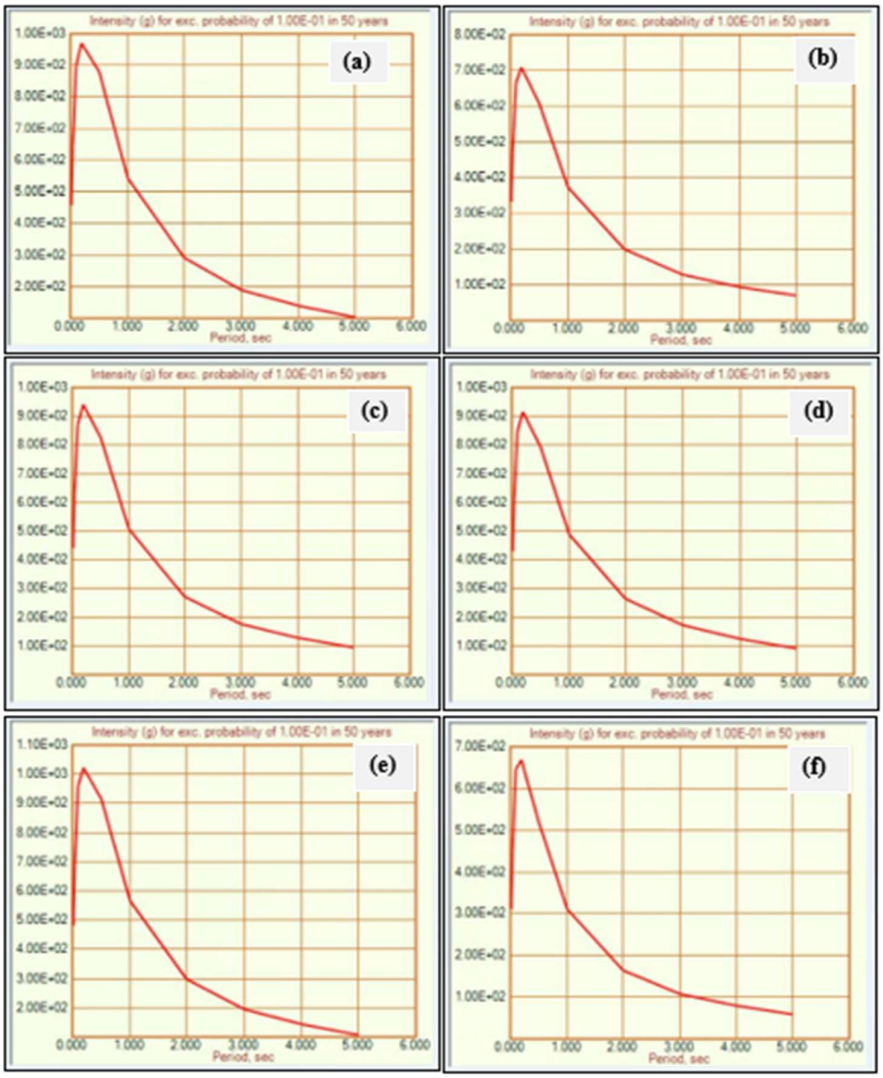
Intensity (g) for exc. probability of 1.00E-01 in 50 years
(a)
(b)
(c)
(d)
(e)
(f)
Period, sec

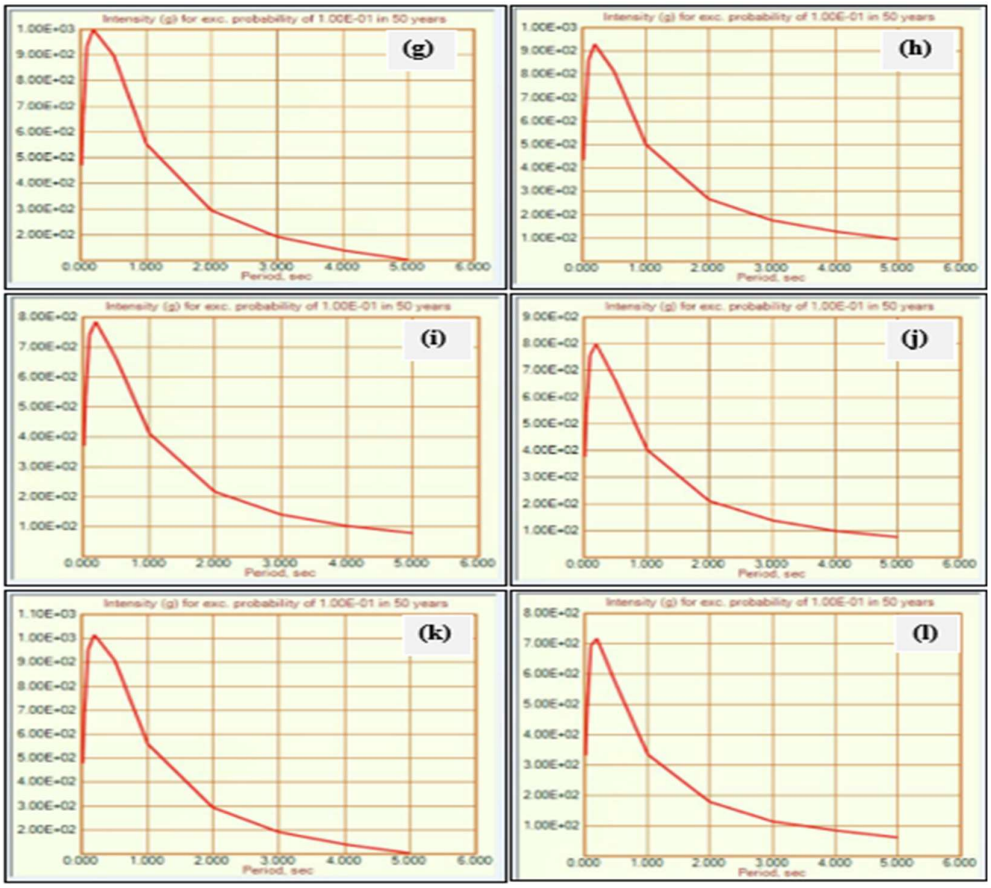

Figure 10. *Site-specific response spectra of the study area (Spectral acceleration (cm/sec^2) vs. Period (sec)); (a) Banga, (b) General Santos City, (c) Koronadal City, (d) Lake Sebu, (e) Norala, (f) Polomolok, (g) Santo Niño, (h) Surallah, (i) T'Boli, (j) Tampakan, (k) Tantangan and (l) Tupi.*

The response spectrum of Banga Municipality that was shown in *Figure 10(a)* is having spectral accelerations of 457 gals or 46.59% of gravity (0.4659g) at time t = 0.01 s, 487 gals (0.496 g) at t = 0.02 s, 643 gals (0.655 g) at t = 0.04 s, 710 gals (0.723 g) at t = 0.05 s, 898 gals (0.915 g) at t = 0.1 s, 971 gals (0.99 g) at t = 0.2 s, 882 gals (0.899 g) at t = 0.5 s, 545 gals (0.556 g) at t = 1.0 s, 291 gals (0.297 g) at t = 2.0 s, 190 gals (0.194 g) at t = 3.0 s, 138 gals (0.141 g) at t = 4.0 s, and 103 gals (0.105 g) at t = 5.0 s, respectively.

Figure 10(b) corresponds to the response spectrum of General Santos City having spectral accelerations of 333 gals or 33.95% of gravity (0.3395g) at time t = 0.01 s, 359 gals (0.366 g) at t = 0.02 s, 472 gals (0.481 g) at t = 0.04 s, 527 gals (0.537 g) at t = 0.05 s, 664 gals (0.677 g) at t = 0.1 s, 710 gals (0.724 g) at t = 0.2 s, 607 gals (0.619 g) at t = 0.5 s, 372 gals (0.379 g) at t = 1.0 s, 199 gals (0.203 g) at t = 2.0 s, 131 gals (0.133 g) at t = 3.0 s, 95.2 gals (0.097 g) at t = 4.0 s, and 71 gals (0.07 g) at t = 5.0 s, respectively.

Figure 10(c) corresponds to the response spectrum of Koronadal City having spectral accelerations of 442 gals or 45.05% of gravity (0.4505g) at time t = 0.01 s, 472 gals (0.481 g) at t = 0.02 s, 627 gals (0.639 g) at t = 0.04 s, 693 gals (0.706 g) at t = 0.05 s, 873 gals (0.890 g) at t = 0.1 s, 940 gals (0.958 g) at t = 0.2 s, 826 gals (0.841 g) at t = 0.5 s, 508 gals (0.518 g)

at t = 1.0 s, 272 gals (0.277 g) at t = 2.0 s, 177 gals (0.180 g) at t = 3.0 s, 129 gals (0.131 g) at t = 4.0 s, and 95.5 gals (0.097 g) at t = 5.0 s, respectively.

Figure 10(d) corresponds to the response spectrum of Lake Sebu Municipality having spectral accelerations of 429 gals or 43.73% of gravity (0.4373g) at time t = 0.01 s, 458 gals (0.467 g) at t = 0.02 s, 609 gals (0.621 g) at t = 0.04 s, 673 gals (0.686 g) at t = 0.05 s, 846 gals (0.862 g) at t = 0.1 s, 915 gals (0.933 g) at t = 0.2 s, 793 gals (0.808 g) at t = 0.5 s, 489 gals (0.498 g) at t = 1.0 s, 263 gals (0.268 g) at t = 2.0 s, 172 gals (0.175 g) at t = 3.0 s, 126 gals (0.128 g) at t = 4.0 s, and 92.9 gals (0.095 g) at t = 5.0 s, respectively.

Figure 10(e) corresponds to the response spectrum of Norala Municipality having spectral accelerations of 483 gals or 49.23% of gravity (0.4923g) at time t = 0.01 s, 521 gals (0.531 g) at t = 0.02 s, 689 gals (0.702 g) at t = 0.04 s, 764 gals (0.779 g) at t = 0.05 s, 961 gals (0.979 g) at t = 0.1 s, 1020 gals (1.04 g) at t = 0.2 s, 918 gals (0.936 g) at t = 0.5 s, 566 gals (0.577 g) at t = 1.0 s, 300 gals (0.305 g) at t = 2.0 s, 196 gals (0.199 g) at t = 3.0 s, 142 gals (0.145 g) at t = 4.0 s, and 106 gals (0.108 g) at t = 5.0 s, respectively.

Figure 10(f) corresponds to the response spectrum of Polomolok Municipality having spectral accelerations of 310 gals or 31.60% of gravity (0.3160g) at time t = 0.01 s, 337 gals (0.344 g) at t = 0.02 s, 451 gals (0.459 g) at t = 0.04 s, 508 gals (0.518 g) at t = 0.05 s, 645 gals (0.657 g) at t = 0.1 s, 669 gals (0.682 g) at t = 0.2 s, 520 gals (0.530 g) at t = 0.5 s, 312 gals (0.318 g) at t = 1.0 s, 165 gals (0.168 g) at t = 2.0 s, 107 gals (0.109 g) at t = 3.0 s, 79 gals (0.081 g) at t = 4.0 s, and 58.6 gals (0.0597 g) at t = 5.0 s, respectively.

Figure 10(g) corresponds to the response spectrum of Santo Niño Municipality having spectral accelerations of 471 gals or 48.01% of gravity (0.480g) at time t = 0.01 s, 504 gals (0.514 g) at t = 0.02 s, 666 gals (0.679 g) at t = 0.04 s, 738 gals (0.752 g) at t = 0.05 s, 933 gals (0.951 g) at t = 0.1 s, 999 gals (1.02 g) at t = 0.2 s, 900 gals (0.917 g) at t = 0.5 s, 554 gals (0.565 g) at t = 1.0 s, 294 gals (0.299 g) at t = 2.0 s, 193 gals (0.197 g) at t = 3.0 s, 140 gals (0.143 g) at t = 4.0 s, and 104 gals (0.106 g) at t = 5.0 s, respectively.

Figure 10(h) corresponds to the response spectrum of Surallah Municipality having spectral accelerations of 435 gals or 44.34% of gravity (0.443g) at time t = 0.01 s, 464 gals (0.473 g) at t = 0.02 s, 617 gals (0.623 g) at t = 0.04 s, 681 gals (0.694 g) at t = 0.05 s, 859 gals (0.876 g) at t = 0.1 s, 929 gals (0.947 g) at t = 0.2 s, 812 gals (0.828 g) at t = 0.5 s, 501 gals (0.511 g) at t = 1.0 s, 270 gals (0.275 g) at t = 2.0 s, 175 gals (0.178 g) at t = 3.0 s, 128 gals (0.130 g) at t = 4.0 s, and 94.6 gals (0.096 g) at t = 5.0 s, respectively.

Figure 10(i) corresponds to the response spectrum of T'Boli Municipality having spectral accelerations of 372 gals or 37.92% of gravity (0.379g) at time t = 0.01 s, 405 gals (0.412 g) at t = 0.02 s, 534 gals (0.544 g) at t = 0.04 s, 602 gals (0.614 g) at t = 0.05 s, 740 gals (0.754 g) at t = 0.1 s, 784 gals (0.799 g) at t = 0.2 s, 663 gals (0.679 g) at t = 0.5 s, 410 gals (0.418 g) at t = 1.0 s, 217 gals (0.221 g) at t = 2.0 s, 142 gals (0.144 g) at t = 3.0 s, 104 gals (0.106 g) at t = 4.0 s, and 78.1 gals (0.079 g) at t = 5.0 s, respectively.

Figure 10(j) corresponds to the response spectrum of Tampakan Municipality having spectral accelerations of 376 gals or 38.32% of gravity (0.383g) at time t = 0.01 s, 409 gals (0.417 g) at t = 0.02 s, 539 gals (0.544 g) at t = 0.04 s, 609 gals (0.621 g) at t = 0.05 s, 757 gals (0.772 g) at t = 0.1 s, 800 gals (0.815 g) at t = 0.2 s, 663 gals (0.676 g) at t = 0.5 s, 405 gals (0.413 g) at t = 1.0 s, 211 gals (0.215 g) at t = 2.0 s, 138 gals (0.141 g) at t = 3.0 s, 100 gals (0.102 g) at t = 4.0 s, and 75 gals (0.076 g) at t = 5.0 s, respectively.

Figure 10(k) corresponds to the response spectrum of Tantangan Municipality having spectral accelerations of 480 gals or 48.93% of gravity (0.498g) at time t = 0.01 s, 517 gals (0.527 g) at t = 0.02 s, 684 gals (0.697 g) at t = 0.04 s, 759 gals (0.774 g) at t = 0.05 s, 954 gals (0.972 g) at t = 0.1 s, 1010 gals (1.03 g) at t = 0.2 s, 910 gals (0.928 g) at t = 0.5 s, 560 gals (0.571 g) at t = 1.0 s, 296 gals (0.302 g) at t = 2.0 s, 194 gals (0.197 g) at t = 3.0 s, 140 gals (0.143 g) at t = 4.0 s, and 105 gals (0.107 g) at t = 5.0 s, respectively.

Lastly, the response spectrum of Tupi Municipality that was shown in the *Figure 10 (l)* is having spectral accelerations of 334 gals or 34.05% of gravity (0.340g) at time t = 0.01 s, 364 gals (0.371 g) at t = 0.02 s, 487 gals (0.496 g) at t = 0.04 s, 551 gals (0.562 g) at t = 0.05 s, 693 gals (0.706 g) at t = 0.1 s, 718 gals (0.732 g) at t = 0.2 s, 566 gals (0.577 g) at t = 0.5 s, 337 gals (0.344 g) at t = 1.0 s, 179 gals (0.182 g) at t = 2.0 s, 116 gals (0.118 g) at t = 3.0 s, 84.7 gals (0.086 g) at t = 4.0 s, and 62.5 gals (0.064 g) at t = 5.0 s, respectively.

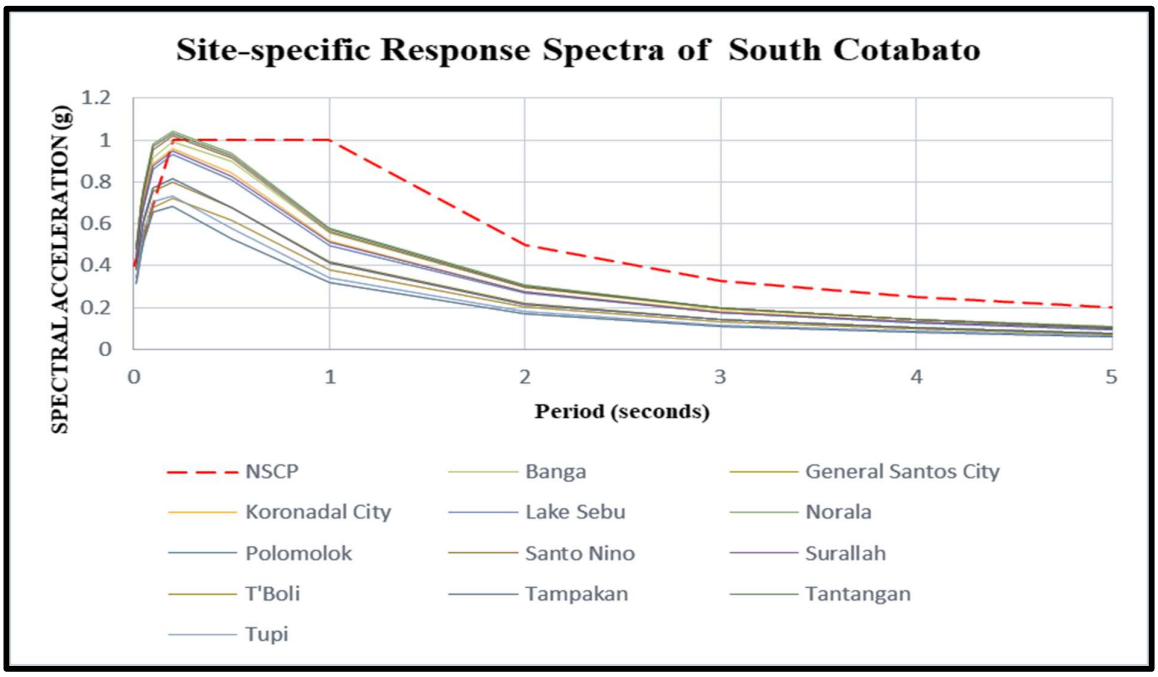

Figure 11. *Site-specific response spectra in the South Cotabato vs. NSCP (2015)*

The site-specific response spectrum of every Municipalities in South Cotabato versus the NSCP recommendation was plotted in *Figure 11*. The result revealed that the peak of the response spectrum from Santo Nino, Norala, and Tantangan was relatively high compare to the NSCP response spectrum. The other Municipalities were resulted relatively low.

CONCLUSION

As a result, at t = 0.01s, Banga, Koronal City, Lake Sebu, Norala, Santo Niño, Surallah, and Tantangan transcend the value of spectral acceleration using at t = 0.00 s of NSCP 2015 response spectrum of 0.4g by 0.466g, 0.451g, 0.437g, 0.492g, 0.48g, 0.44g, and 0.489g, respectively. On the other hand, General Santos City, Polomolok, T'Boli, Tampakan, and Tupi are of lesser value than of NSCP response spectrum at t = 0.01s by 0.34g, 0.316g, 0.379g, 0.383g, and 0.340g, respectively. The response spectrum developed from the PSHA generally provides a better response spectrum for site response analysis. The primary reason is that the

spectral ordinates of the response spectra were developed by GMPE's directly in the PSHA that gives a more realistic response shape.

Moreover, the hazard maps and model presented here may be used to enhance appropriate and site-specific seismic capacity of future engineered structures and related facilities to improve building resilience and safety of occupants to future intense earthquakes, considering acceptable risks and engineering economy. Designers can ensure their structures can withstand a given level of ground shaking while maintaining a desired level of performance using the generated site-specific response spectra. This information may be used as a basis for seismic provisions in building codes, budget allocations for risk reduction, and risk models used for municipalities and the Province of South Cotabato.

REFERENCE

1. Adagunodo, T. A., & Sunmonu, L. A. (2015). Earthquake : A terrifying of all natural phenomena. *Journal of Advances in Biological and Basic Research*, *1*(June), 4–11.
2. Ahmad, N. (2016). *[Document Improved Version]: Steps for Conducting Probabilistic Seismic Hazard Analysis using GIS and CRISIS Tools*. *December*.
3. Anbazhagan, D. P. (2017). *Introduction to Engineering Seismology Lecture 12*. 1–34.
4. Atkinson, G. M., & Boore, D. M. (2006). Earthquake ground-motion prediction equations for eastern North America. *Bulletin of the Seismological Society of America*, *96*(6), 2181–2205. https://doi.org/10.1785/0120050245
5. Baguhin, I. A., & Orejudos, J. N. (2020). *Site-Specific Response Spectra : 2 nd District of Cagayan de Oro City , Philippines*. *18*(1), 93–117.
6. Bajaj, K., & Anbazhagan, P. (2019). Regional stochastic GMPE with available recorded data for active region – Application to the Himalayan region. *Soil Dynamics and Earthquake Engineering*, *126*(August), 105825. https://doi.org/10.1016/j.soildyn.2019.105825
7. Boore, D. M., Thompson, E. M., & Cadet, H. (2011). *Regional Correlations of VS30 and Velocities Averaged Over Depths Less Than and Greater Than 30 Meters Regional Correlations of V S 30 and Velocities Averaged Over Depths Less Than and Greater Than 30 Meters*. *October 2014*. https://doi.org/10.1785/0120110071
8. Borcherdt, R. D. (2010). *V S30 – A Site-Characterization Parameter for Use in Paper Title Line Simplified Building Codes , Earthquake Resistant Design , GMPEs , and ShakeMaps ?? Paper Title Line 2*. *10*(2010).
9. Cornell, B. Y. C. A. (1968). Engineering Seismic Risk Analysis. *Bulletin of the Seismological Society of America*, *58*(5), 1583–1606.
10. Felzer, K. (2006). Calculating the Gutenberg-Richter b value. *AGU Fall Meeting Abstracts*, *1*, 8.
11. Gardner, J. K., & Knopoff, L. (1974). Is the Sequence of Earthquakes in Southern California, with Aftershocks Removed, Poissonian? *Bulletin of the Seismological Society of America*, *64*(5), 1363–1367. http://citeseerx.ist.psu.edu/viewdoc/download?doi=10.1.1.467.2509&rep=rep1&type=pdf
12. Jhinkwan, H., & Jain, P. K. (2016). *PREDICTION OF SHEAR WAVE VELOCITY USING SPT – N VALUE*. *7*, 28–36.

13. Johnson, K. L., Perez, J. S., Bonita, J. D., Ishmael, C., Jr, R. U. S., Pagani, M. M., & Allen, T. I. (2020). *Probabilistic seismic hazard analysis model for the*. https://doi.org/10. 1177/ 8755293019900521
14. Kalkan, E., S.M.EERI, Lkan, P. G., & M.EERI. (2004). *Site-Dependent Spectra Derived from Ground Motion Records in Turkey*. *20*(4), 1111–1138. https://doi.org/10.1193/1.1812555
15. Nbazhagan, P. A., Umar, A. B. K., & Itharam, T. G. S. (2013). *Seismic Site Classification and Correlation between Standard Penetration Test N Value and Shear Wave Velocity for Lucknow City in Indo-Gangetic Basin*. *170*, 299–318. https://doi.org/10.1007/s00024-012-0525-1
16. Ordas, M., & Salgado-Gálvez., M. A. (2017). *R-CRISIS Validation and Verification Document. Technical Report. Mexico City, Mexico.*
17. Ordaz, M., & Salgado-Gálvez., M. A. (2017). *R-CRISIS MANUAL*.
18. WRR. (2022). *WorldRiskReport 2022*. 1–71. https:// https://weltrisikobericht.de/wp-content/uploads/2022/09/WorldRiskReport-2022_Online.pdf
19. Wyss, M., Wiemer, S., & Zúñiga, R. (2001). ZMAP A TOOL FOR ANALYSES OF SEISMICITY PATTERNS TYPICAL APPLICATIONS AND USES : A COOKBOOK Table of Content. *Writing*, 64.